Cooperative Slowdown of Water Rotation Near Densely Charged Ions is Intense but Short-Ranged

Ana Vila Verde[*,†,‡] and Reinhard Lipowsky[*,†]

Max Planck Institute of Colloids and Interfaces, Theory and Bio-Systems Department, Wissenschaftspark Golm, 14424 Potsdam, Germany;

E-mail: ana.vilaverde@mpikg.mpg.de; Reinhard.Lipowsky@mpikg.mpg.de

[*]To whom correspondence should be addressed

[†]Max Planck Institute of Colloids and Interfaces, Theory and Bio-Systems Department, Wissenschaftspark Golm, 14424 Potsdam, Germany;

[‡]Also at the University of Minho, Physics Center, Campus de Gualtar, 4710-057 Braga, Portugal.

Abstract

We investigate the reorientation dynamics of water at 300 K in solutions of magnesium sulfate and cesium chloride from classical atomistic molecular dynamics simulations using the "simple water model with four sites and negative Drude polarizability" (SWM4-NDP) and accompanying ion models; for SO_4^{2-}, we derive SWM4-NDP-compatible parameters. Results indicate that pairs of ions have a cooperative effect on water rotation, but do not support the model based on experiment whereby ion cooperativity increases the number of very slow water molecules well beyond the ions' first hydration shell. Instead, we find that cooperative slowdown beyond the first hydration shell is weak. Intense cooperative slowdown is limited to the first hydration shells, the magnitude of the slowdown being stronger for the multivalent ions. Cooperative effects for different salts differ in both the magnitude of rotational slowdown and the spatial range of the affected water subpopulations.

Keywords: water rotation; Hofmeister; inorganic ions; cooperativity; ion hydration; ion-specific effects; magnesium sulfate

1. Introduction

Understanding the structure and dynamics of water in solutions containing small, inorganic ions is essential to understand many different processes occurring in systems as diverse as atmospheric aerosols, land water masses, or living organisms. It has been known for decades that different salts have different relative ability to alter properties of aqueous salt solutions or of ternary systems (water+salt+other solute), for example, to increase the surface tension of solutions, to tune protein denaturation temperatures or to alter the stability of colloid suspensions[1]. A series of anions or cations ranked by the magnitude of their effect on a given property is termed a Hofmeister series. Because Hofmeister series obtained for widely different properties are very similar, the interactions between ions and water are thought to be, at least partially, at the origin of these series[2–7].

Over the past decade, multiple experimental and simulation studies have investigated the structure and picosecond dynamics of water in solutions of ions[8–21]. Most studies suggest that the effect of anions and cations with low charge density on water structure and dynamics is largely limited to their first hydration shell. The exception to this trend is found for ions with large charge density such as Li^+, SO_4^{2-}, or Mg^{2+}, which appear to perturb the structure and/or dynamics of a larger number of water molecules.

One still unresolved issue is the extent, to which the effect of one ion on the dynamics of water depends on the counter-ion – i.e., the extent, to which the effect of anion and cation on water dynamics are cooperative – and the related issues of (i) the spatial range and the magnitude of the cooperative slowdown and (ii) the connection between cooperative effects and the characteristic length scales of anion-cation interactions. Recent experiments that addressed these issues have led to rather different conclusions. Some recent femtosecond infrared spectroscopy (fs-IR) and dielectric relaxation (DR) studies indicate that densely charged ions have strongly cooperative effects on the rotational dynamics of water and that these effects extend much beyond the first hydration shell of the ions[22,23]. This conclusion was drawn from a two-population model according to which water molecules in aqueous so-

lutions of any inorganic salt have either bulk-like dynamics, with reorientation time 2.6 ps, or slow dynamics, with reorientation time 10 ps. Differences in the measured reorientation decay of various salt solutions then reflect the different *number* of water molecules slowed down by each salt, not changes in the *magnitude* of that slowdown. Other studies using similar techniques and systems do not support this picture[20,24,25] and indicate that strong cooperative slowdown occurs only in the first hydration layer of the ions[20]. This latter scenario is supported by the only simulation study published to date that specifically investigated the rotational dynamics of different water subpopulations in aqueous solutions of simple, inorganic ions[26]. This simulation study relied, however, on simplistic models for solutions of 1:1 (the magnitude of the cation:anion charges) inorganic ions, for which cooperative slowdown effects, if present, are expected to be weaker[23,27]. Resolving this controversy is important to better understand the origin of Hofmeister series and also has significant practical implications. For example, it would be interesting to investigate the form and extent to which cooperative effects on water dynamics connect with long-range ion-water and ion-ion structural correlations. Long-range structural effects are negligible for monovalent salts, and thus coarse-grained models of ions that do not account for ion-ion correlations can still successfully explain specific-ion effects such as the variation of the critical coagulation concentration of hydrophobic colloidal suspensions[28] or the effects of ions on the surface tension of aqueous solutions[29] of monovalent salts. Similar models might be less successful for salts of multivalent ions. Cooperative effects of ions on water dynamics would also impact the development of less simplistic models based on the Generalized Langevin Equation (GLE). This category of models is indispensable to investigate long timescale ion transport processes that are currently not accessible to all-atom simulations[30–32]. Long-range cooperative effects on water dynamics would imply that the ion-ion memory kernels necessary for the GLE should depend on the interionic distance even for large interionic separations, if the aim is to adequately describe system dynamics.

In this Letter, we address the controversy surrounding cooperative effects of ions on water

reorientational dynamics by using molecular dynamics simulations and polarizable models to investigate the rotational dynamics of water in aqueous solutions of magnesium sulfate and cesium chloride. Magnesium sulfate induces the largest cooperative slowdown observed in experiment, whereas for cesium chloride only weak effects have been found[22,23]. In what follows, we examine how individual pairs of ions at different anion-cation separations affect the reorientation of water OH groups and water dipoles, and assess the extent and magnitude of cooperative slowdown in these systems by comparison with isolated ions. Cooperative slowdown in systems with multiple nearby ion pairs, typical of concentrated solutions, is also compared with that near individual ion pairs. The theoretical foundation for the approach used in this study – simulations using polarizable models including a newly developed set of parameters for SO_4^{2-}– are presented in the Methods section.

Methods

As mentioned above, our study uses molecular dynamics simulations and classical, polarizable, models to investigate cooperative effects of magnesium sulfate and cesium chloride salts on the rotational dynamics of water molecules. Densely charged ions like Mg^{2+} or SO_4^{2-} strongly polarize water molecules in their first hydration shell[33,34]. Because this effect has been shown to strongly affect the dynamics of these water molecules[35], we opt for polarizable models for this study. We use the "simple water model with four sites and negative Drude polarizability" (SWM4-NDP) and associated models for Mg^{2+}, $Cl^-$and Cs^+[36,37]. Polarization is explicitly included in these models through classical Drude oscillators. For SO_4^{2-}, we develop parameters fully compatible with the SWM4-NDP model. A complete description of the procedure used to parameterize SO_4^{2-} is given in the Supporting Information. The water model reproduces, with a maximum error of 10%, the change in internal energy upon liquefaction, molar volume, diffusion coefficient, relaxation time from nuclear magnetic resonance measurements, dielectric constant, free energy of hydration and surface tension

determined from experiment at 298 K.[36] The polarizable models for ions used in this work were optimized to reproduce properties that reflect water-ion interactions: the free energies of hydration[38] of these ions and the minimum energy and ion–water oxygen distance of monohydrate (1 water + 1 ion) systems[39], while requiring that the total sulfate polarizability remain within physically reasonable bounds[40–42]. The correction terms necessary when calculating free energies in systems with periodic boundary conditions were used[37,43–45]. For Mg^{2+}, $Cl^{-}$and Cs^{+}, the model yields estimates of the position of the first and second maxima of the ion-water oxygen radial distribution function, the number of waters in the first hydration layer of these ions and the diffusion coefficients of salts consistent with experimental and ab initio data[37,46,47]. The position of the first peak of the SO_4^{2-}-water oxygen radial distribution function, the number of waters in the first hydration shell of the sulfate and the spatial range of structurally perturbed water are within the range of reported values from tracer diffusion measurements, X-ray, infrared photodissociation spectroscopy, ab initio or molecular dynamics simulations[18,39,40,48–51]. The overall quality of the water and ion models makes them a suitable choice for this study.

The simplest system where cooperative effects of ions on water rotation may arise is an individual anion-cation pair. Because solutions of low to moderate ($\simeq$1 M) concentrations consist mainly of quasi-isolated ions and ion pairs[52], experimental observations of cooperativity at these concentrations have been interpreted as resulting from the effect of isolated pairs of ions on water dynamics. We thus focus our attention on these systems. Cooperative slowdown of water rotation in these systems is necessarily a function of the characteristic configurations assumed by the ions: contact ion pairs (CIPs) if the two ions come in direct contact, solvent-shared ion pairs (SIPs) if the ions share one water layer, and solvent-separated ion pairs (2SIP) if they share two water layers[52]. Dielectric relaxation studies[52] indicate that ion pair structures in aqueous solutions of magnesium sulfate are long-lived, having lifetimes at least comparable to their rotational correlation time: $\tau_{CIP} \approx 20$ ps, $\tau_{SIP} \approx 115$ ps and $\tau_{2SIP} \approx 300$ ps. Because these timescales are typically much larger than

those associated with the rotation of water hydroxyl groups or water dipoles (1-10 ps)[22], the ion configurations can be considered essentially fixed over the timescales of water reorientation. We take advantage of this separation of timescales and opt to perform molecular dynamics simulations with ions at fixed anion-cation distances. This approach has the advantage of eliminating the largest source of uncertainty from our study: the model's ability to capture the correct anion-cation association behavior. Prior studies have shown that ion models that, like the ones used here, are parameterized using water-ion properties, can successfully be used to investigate other properties of water near ions, but often lead to an unreliable description of anion-cation association[35,53–57]. To assess the effect of individual pairs of ions on water dynamics, we carry out simulations of single pairs of ions in fixed configurations, with anion-cation distances assuming the values $D = 5, 6, 8, 10, 12$ Å. A typical initial configuration used for the simulations is shown in Figure 1(a). $D = 5, 6$ Å correspond to solvent-shared and solvent-separated configurations[52], respectively; $D = 12$ Å corresponds to the average ion-ion distance for a 0.5 M solution. Distances below 5 Å, corresponding to contact ion pair configurations, are not investigated because other simulation studies indicate that CIP configurations have very limited effect on water dynamics[26], and because dielectric relaxation, Raman and heat of dilution studies indicate that CIPs should not be the dominant species in magnesium sulfate solutions up to moderate concentrations[52,58–61].

At concentrations much higher than 0.5 M, however, a non-negligible fraction of ion pairs will be near other ion pairs. We gain insight into the effect of multi-ion configurations on water dynamics by performing simulations where tens of fixed ions at different anion-cation distances coexist in a simulation box. A representative configuration used for the simulations is shown in Figure 1(b). Below we discuss how the fixed ion configuration used in these simulations affects our interpretation of these results.

Evaluating the extent to which either individual pairs of ions or multi-ion systems *cooperatively* slow down water rotational dynamics requires that we compare the dynamics of water in these systems against water dynamics in systems with isolated ions. The effect of isolated

ions on water dynamics is obtained from simulations where four cations and four anions are placed in fixed positions in the simulation box so that the minimum distance between any two ions is $D \simeq 23$ Å. This large separation ensures that the static and dynamic properties of water near an ion are unaffected by the remaining ions. The initial configuration used for the simulations with isolated ions is shown in Figure 1(c).

We perform all-atom molecular dynamics simulations using the molecular dynamics package NAMD[62]. The package VMD – Visual Molecular Dynamics – is used to visualize and analyze trajectories[63]. Electrostatic interactions are calculated using the standard Coulomb relation up to 12 Å and using the Particle Mesh Ewald method with 1 Å grid-spacing for larger separation. Van der Waals (VdW) interactions are smoothly switched to zero between 10 and 12 Å, and long-range corrections for the energy and pressure are used. The Brünger-Brooks-Karplus algorithm with multiple time stepping is used for integration, with bonded and VdW forces calculated every 0.5 fs and electrostatic forces every 1 fs. Classical dynamic trajectories near the self-consistent field limit are generated using extended Lagrangian dynamics with a dual-Langevin thermostat[64]. The SETTLE algorithm is used to fix the geometry of the four non-Drude particles of the water molecule[65]. Periodic boundary conditions are used. Simulations are equilibrated for 2 ns in the NPT ensemble. During this stage, the constant pressure requirement is satisfied through a Langevin barostat with a target pressure 1 atm, oscillation period 100 fs and damping timescale 50 fs. The target temperature for the Drude thermostat is 1 K and for the remaining degrees of freedom it is 300 K. Both thermostats use a damping coefficient of 5 ps^{-1}. Production runs are performed in the canonical (NVT) ensemble using a damping coefficient of 0.1 ps^{-1} for the Drude pairs and 0.05 ps^{-1} for the overall system. Previous studies indicate that these damping constants lead to diffusive behavior indistinguishable from that obtained using simulations in the microcanonical ensemble. A single production run lasting 2.5 ns is carried out for the systems with isolated ions. For the systems with single ion pairs, 20 production runs each 5 ns long are performed for each anion-cation separation, totalling 100 ns for each anion-cation sepa-

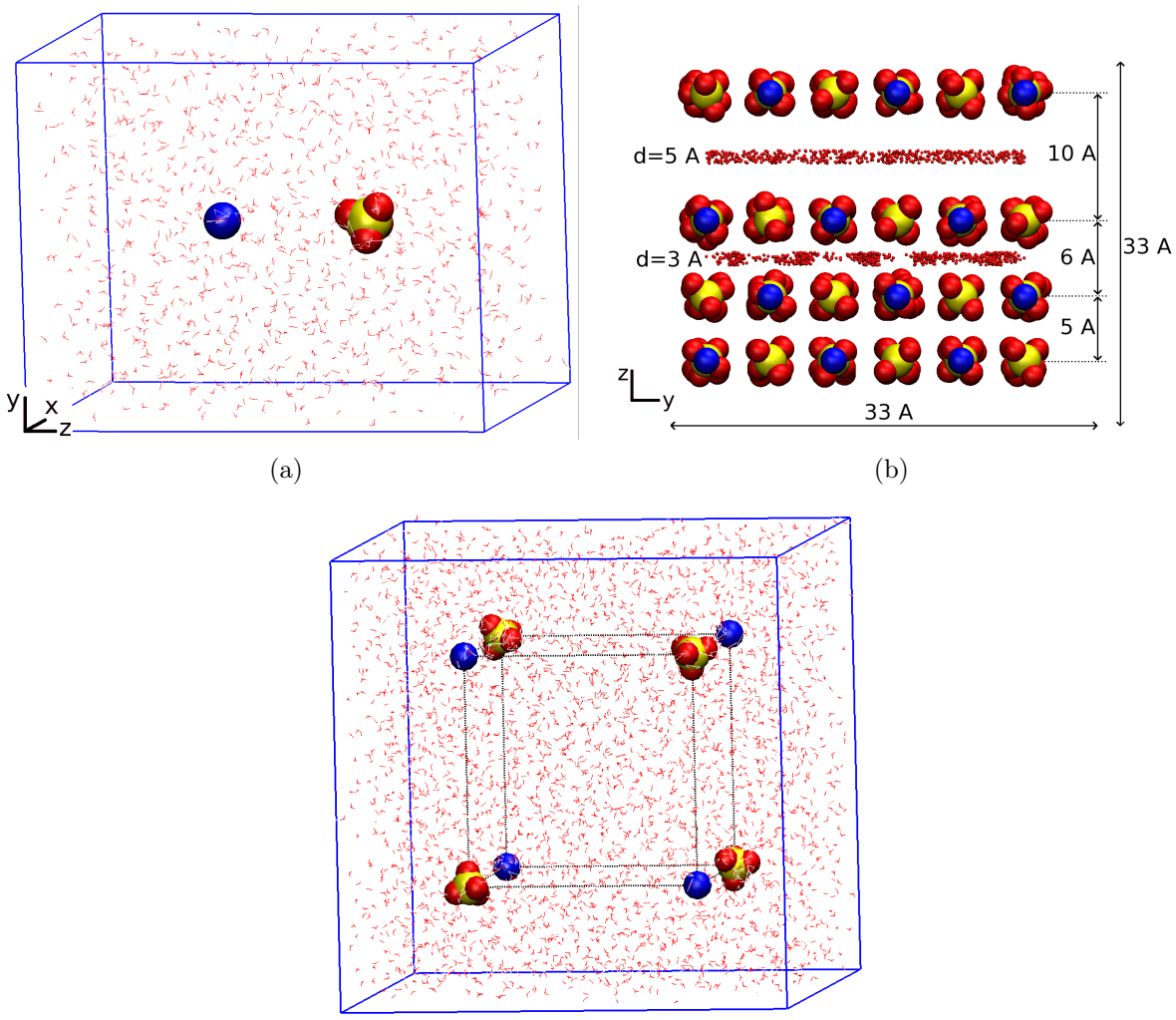

(a) (b)

(c)

Figure 1: Geometry of the simulated systems after equilibration, shown here for magnesium sulfate. (a) Individual ion pairs: box dimensions are $29 \times 29 \times 36$ Å^3; the system consists of 1040 water molecules and one ion pair; the anion-cation distance assumes the values 5, 6, 7, 8, 10 or 12 Å. (b) Multiple ion pairs: box dimensions are $33 \times 33 \times 33$ Å^3; the system consists of 1126 water molecules and 72 pairs of ions; in the XY plane the Mg^{2+} and SO_4^{2-} ions are in alternated positions spaced by 5 Å. $d = 3$ and $d = 5$ Å designate the two water subpopulations represented by the small red points for which the water dynamics is characterized. Other water molecules in the system are not shown. (c) Isolated ions: box dimensions are $47 \times 47 \times 47$ Å^3; the system consists of 3448 water molecules and four pairs of ions; the minimum anion-cation distance is 23 Å.

ration. Such long simulation times are necessary to ensure that the reorientation dynamics of small water subpopulations at different locations in the simulation box are adequately sampled. For the multi-ion systems, five production runs each 5 ns long are performed,

totalling 25 ns. The average temperature during the production runs is $T = 300 \pm 5$ K. Unless otherwise indicated, the statistical uncertainty of reported quantities is estimated by calculating the standard deviation using block averages[66,67].

3. Results and Discussion

We first investigate the reorientation of different subpopulations of water molecules in systems with a single pair of ions. The criteria used to select these subpopulations are illustrated in Figure 2(a): at $t = 0$, water oxygens must both belong to a hollow sphere of radius d and thickness 1 Å centered at one of the ions, and to a slab of thickness 0.5 Å perpendicular to the cation-anion direction and at different positions along that direction. The position of the slab is characterized by an angle θ_{ion}, where the subscript indicates the ion at the vertex of the angle as shown in Figure 2. Each water subpopulation is thus identified by the triad (ion, d, θ_{ion}). We note that the sulfate is tetrahedrally symmetric implying that different water subpopulations centered on that ion should display heterogeneous structure and dynamics around the anion-cation axis. Our definition of water subpopulations averages over any such heterogeneity near sulfate so we can focus on differences in water reorientation arising from differences in the initial distance of water molecules to either ion. For the cesium chloride system, water subpopulations will have structure and dynamics that are radially symmetric around the anion-cation axis.

For each subpopulation, we characterize the rotational motion of OH groups and of the water dipole using the second order rotational autocorrelation function

$$P_{2,x}(t) = \langle \frac{1}{2} \Big(3\cos^2(\vec{u}_0 \cdot \vec{u}_t) - 1 \Big) \rangle \tag{1}$$

In this function, $\vec{u}_t$ is the unit vector characterizing the orientation of a OH group or a water dipole in the coordinate frame of the simulation box at time t; the average is over all time origins and an ensemble of molecular groups indicated by x ($x = OH$ or $x = dip$ for hydroxyl

groups or water dipoles, respectively). The function has a maximum with $P_2 = 1$ indicating perfect orientation correlation, and a minimum with $P_2 = -0.5$ when all OH groups form a 90° angle with their initial orientation; in the limit of full, isotropic, 3D decorrelation, $P_2 = 0$. We select this particular function because it approximates the rotational anisotropy decay of OH groups measurable from pump-probe spectroscopy[68]. Because $P_{2,OH}(t)$ neglects non-Condon effects, excited-state absorption and spectral diffusion, this function tends to overestimate the loss of orientation correlation detected in experiment[68]. For this reason, we make only qualitative comparisons between our results and experiment. We note that the autocorrelation function is calculated for the water OH groups ($P_{2,OH}(t)$) and for the water dipole ($P_{2,dip}(t)$) of those water molecules, irrespective of their position in the simulation box at time t. Within the 20 ps time interval over which P_2 is calculated, water molecules initially in the first and second hydration layers of Mg^{2+} and in the first hydration layer of SO_4^{2-} largely remain at those locations because they have residence times much larger than or comparable to 20 ps (see Supporting Information). Water molecules initially in the outer hydration layers of Mg^{2+} or SO_4^{2-}, or in any of the hydration layers of Cs^+ or Cl^-, have residence times of order $\simeq$ 10 ps, indicating that over 20 ps they may diffuse to the immediately adjacent hydration layers.

For each of the two ions, $P_{2,OH}(t)$ and $P_{2,dip}(t)$ are calculated for all possible combinations of d =2, 3, $\cdots$, 12 Å and θ =0, 45, 60, 90, 180°. The $P_{2,OH}(t)$ and $P_{2,dip}(t)$ curves, a few of which are shown in Figure 3, display the expected[26,68–71] fast, non-exponential decay for $t < 200$ fs, followed by bi-exponential decay at picosecond timescales. The initial fast loss of orientation correlation is due to librational motion whereas the later decay reflects structural change[68,69,71,72]. Studies of water in the bulk, in solutions and at a variety of interfaces by Laage, Hynes and co-workers[69,73–79] and others[70,71] indicate that, for $P_{2,OH}(t)$ curves, the later decay results from at least two processes: hydrogen bond breaking and reformation (also termed hydrogen bond exchange) and slow reorientation of the O–H$\cdots$O atom triad without hydrogen bond exchange. Because it is reasonable to expect that

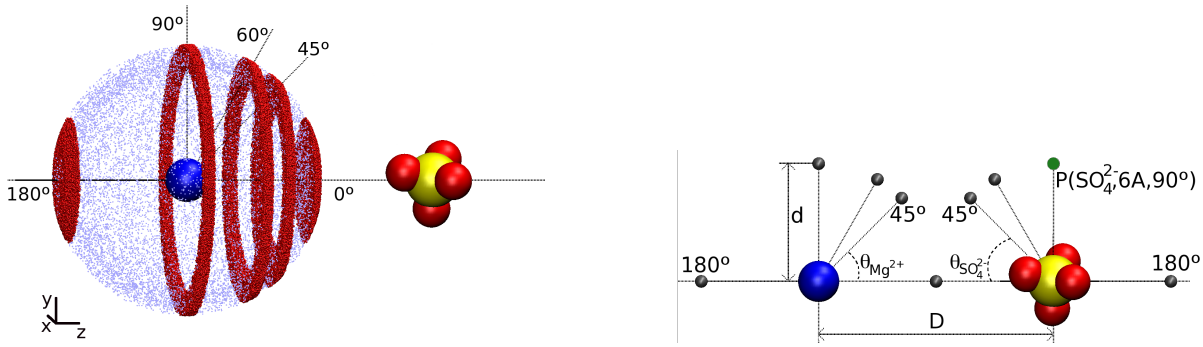

(a) (b)

Figure 2: (a) Water subpopulations (small red dots) near a pair of ions and for which the reorientation dynamics is characterized. For clarity, only water subpopulations centered on magnesium are shown but analogous subpopulations centered on sulfate are also investigated. (b) The different water subpopulations near a pair of ions separated by distance D are schematically represented by the gray spheres, and identified in the text by the reference ion, distance d and angle θ that characterize them, as illustrated for point P (green).

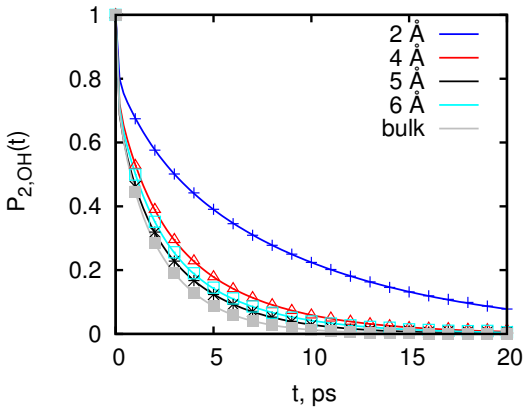

Figure 3: Reorientation decay of OH groups in water subpopulations $(Mg^{2+}, 2-6\text{Å}, 0°)$ in the system with Mg^{2+}-SO_4^{2-}separation $D = 12$ Å. The points are from the simulations, the lines are fits of a sum of three exponentials as described in the text.

the same three processes occur for water near ions, we fit a sum of three exponentials $a\exp(-t/\tau_1) + b\exp(-t/\tau_2) + c\exp(-t/\tau_3)$ to each $P_{2,OH}(t)$ and $P_{2,dip}(t)$ curve. We note, however, that we make no attempt to explicitly connect each of the three time constants extracted from the fit to a particular physical process. A sum of three exponentials is simply a convenient functional form that adequately fits the calculated autocorrelation functions, as illustrated in Figure 3. To facilitate comparisons of the reorientational decay across multiple

water subpopulations, we then calculate the average reorientation decay time,τ_x, for each ensemble of molecular groups x, as the weighted sum of the six fitting parameters τ_1, τ_2 and τ_3 and a, b, c, via $\tau_x \equiv (a\tau_1 + b\tau_2 + c\tau_3)/(a + b + c)$. The resulting time constant can be interpreted as that associated with a single exponential function with the same value at $t = 0$ and with the same area under the curve as the fitted function.

Following this procedure, we obtain the average time constants characterizing reorientation of different water subpopulations near individual cation-anion pairs. In Figure 4(a) we graphically represent the results of this calculation for the case of reorientation of OH groups near a Mg^{2+}-SO_4^{2-} pair separated by $D = 12$ Å. The time constants, τ_{OH}, are shown as a function of the (ion, d, θ_{ion}) triad that characterizes each water subpopulation; see Figures 2(a) and 2(b) for an explanation of the schematic representation. The time constants shown in Figure 4(a) indicate that water rotation near ions slows down relative to the bulk, in line with prior reports[22,25–27,80,81]. The water molecules showing the slowest reorientation are those in the first hydration layer of Mg^{2+}, followed by those in the first hydration layer of SO_4^{2-}. More importantly, the time constants have a weak angular dependence, with water subpopulations between the ions ($\theta < 90°$) showing slightly larger reorientation times than water subpopulations at the same distance from the ion but with $\theta > 90°$. This angular dependence suggests that magnesium sulfate cooperatively slows down water rotation. Comparison of the time constants of the (Mg^{2+},6Å,0°) and the (Mg^{2+},6Å,90°) subpopulations (2.3 ps vs. 1.9 ps) indicates that this effect is weak, but long-range.

We determine the magnitude of cooperative slowdown by comparing the reorientational decay of OH groups and water dipoles for each (ion, d, θ_{ion}) water subpopulation in systems with pairs of ions, with the reorientational decay for the corresponding water subpopulation near the *isolated* cation or anion. Because the systems with isolated ions are radially symmetric, the corresponding subpopulation forms a hollow sphere with radius d and thickness 1 Å, centered on the same ion. Following a procedure entirely analogous to that described above for simulations with pairs of ions, we obtain the average decay times, $\tau_{isol,x}$, of the

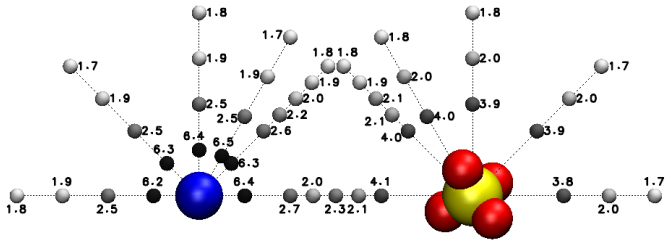

(a) τ_{OH} (ps).

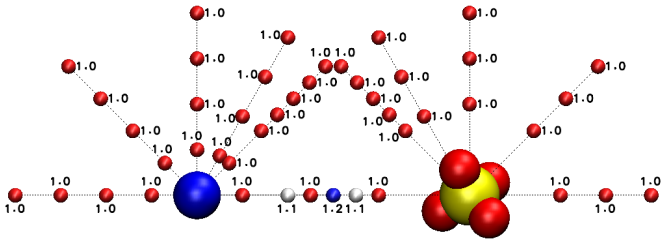

(b) Cooperative slowdown factors ($f_{c,OH}$) for OH rotation.

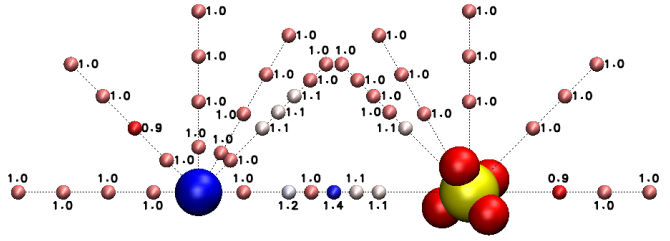

(c) Cooperative slowdown factors ($f_{c,dip}$) for dipole rotation.

Figure 4: Reorientation dynamics of different water subpopulations near a single Mg^{2+}-SO_4^{2-} pair at $D = 12$ Å separation. The numbers next to the small spheres represent the average reorientation times, τ_{OH}, in (a), and the cooperative slowdown factors, $f_{c,x}$, calculated using Equation 2, in (b),(c). The color of the small spheres in each panel encodes the magnitude of the reorientation time or the cooperative slowdown factor shown next to each sphere. Consecutive water subpopulations along the dotted lines are 1 or 2 Å apart.

ensemble of molecular groups x of each water subpopulation near an isolated ion; all $\tau_{isol,x}$ are given in the Supporting Information. The magnitude of cooperative slowdown is then quantified by the cooperative slowdown factor, $f_{c,x}$, defined as the ratio

$$f_{c,x} = \frac{\tau_x}{\tau_{isol,x}} \tag{2}$$

between the average reorientation decay time (τ_x) for water OH groups or water dipoles of water subpopulations in a system with pairs of ions, and the decay time ($\tau_{isol,x}$) of the

corresponding subpopulation for the system with an isolated ion. A cooperative slowdown factor $f_{c,x} = 1$ indicates absence of any cooperative effects of the anion and cation on water dynamics; $f_{c,x} > 1$ indicates cooperative slowdown of water rotation, whereas $f_{c,x} < 1$ indicates cooperative speedup.

The cooperative slowdown factor, $f_{c,x}$, associated with the reorientation of water OH groups or water dipoles is shown for the system with Mg^{2+} and SO_4^{2-} separated by 12 Å in Figures 4(b) and 4(c). The cooperative slowdown factors for water subpopulations equidistant from either ion are calculated twice, using $\tau_{isol,x}$ for both ions. In most equidistant configurations, the same cooperative slowdown factor is obtained and so only one value is shown. For a 12 Å anion-cation separation, the reorientation dynamics of water in the first hydration layer of the ions ($d = 2$ Å for Mg^{2+}, $d = 4$ Å for SO_4^{2-}) is identical within statistical uncertainty to that near the isolated ions, as indicated by $f_c = 1 \pm 0.1$. In contrast, long-range cooperative slowdown is seen for water subpopulations *further* from either ion but directly between them, at $\theta = 0°$ and $d = 6$ Å. The presence of weak but long-range cooperative slowdown for Mg^{2+}-SO_4^{2-} at large separations is qualitatively in line with recent simulation studies that indicate that highly charged ions can induce weak but long-range changes in the average number of hydrogen bonds accepted or donated by water molecules[21], a factor that directly influences rotation of water molecules[74]. For the small water subpopulation half way between Mg^{2+} and SO_4^{2-}, the cooperative slowdown factors are $f_{c,OH} = 1.2$ and $f_{c,dip} = 1.4$. Qualitatively similar results are obtained for the magnesium sulfate system with 10 Å separation between anion and cation, as shown in the Supporting Information. At the same anion-cation separations, cooperative slowdown effects are not observed for the cesium chloride system as shown in Figure 5 for $D = 12$ Å and in the Supporting Information for $D = 10$ Å.

We now examine the cooperative slowdown factors for OH and dipole reorientation, for the systems with anion-cation separation below 10 Å. We first consider the shortest Mg^{2+}-SO_4^{2-} separation, 5 Å, corresponding to a solvent-shared ion pair. As shown in Figure 6,

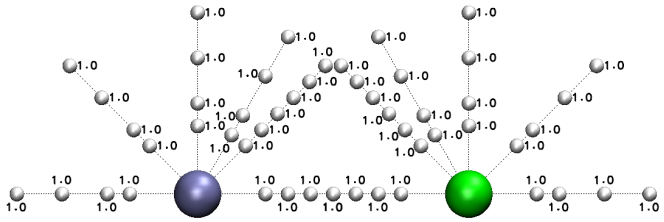

(a) Cooperative slowdown factors for OH rotation, $f_{c,OH}$.

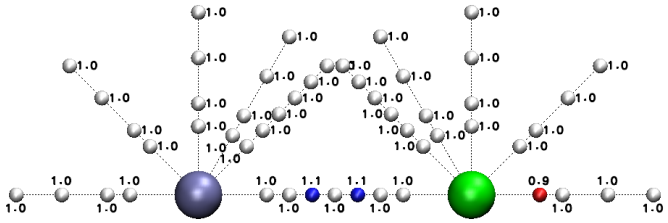

(b) Cooperative slowdown factors for dipole rotation, $f_{c,dip}$.

Figure 5: Reorientation dynamics of different water subpopulations near a single Cs^+-Cl^- pair at $D = 12$ Å separation. The numbers next to the small spheres represent the cooperative slowdown factors, $f_{c,x}$, calculated using Equation 2. The color of the small spheres in each panel encodes the magnitude of the cooperative slowdown factor. Consecutive water subpopulations along the dotted lines are 1 or 2 Å apart.

this small anion-cation separation induces markedly different effects from those described above. This configuration induces intense cooperative slowdown of rotation of OH groups (Figure 6(a)) and of water dipoles (Figure 6(b)), with maximum cooperative slowdown factors of $f_{c,OH} = 6.2$ and $f_{c,dip} = 3.1$. At this anion-cation separation, maximum cooperative slowdown is observed for water in the first hydration layer of Mg^{2+} ($d = 2$ Å) and for the water subpopulations located at $\theta = 45°$. In addition, a 5 Å anion-cation separation induces significant differences in the cooperative slowdown effect between the anion and the cation that are not present for larger anion-cation separations. First, much larger cooperative slowdown is seen for water in the first hydration layer of Mg^{2+} (e.g. for (Mg^{2+},2Å,60°), $f_{c,OH} = 3.2$) than of SO_4^{2-} (e.g. for (SO_4^{2-},4Å 60°), $f_{c,OH} = 1.5$). Second, significant differences are also observed between the two measures of rotation considered here: rotation of water dipoles vs. rotation of OH groups. Whereas cooperative rotational slowdown of water dipoles near SO_4^{2-} only occurs for those water subpopulations between the two ions ($\theta_{SO_4^{2-}} < 90°$), for Mg^{2+} intense cooperative slowdown of dipole rotation occurs in the entire

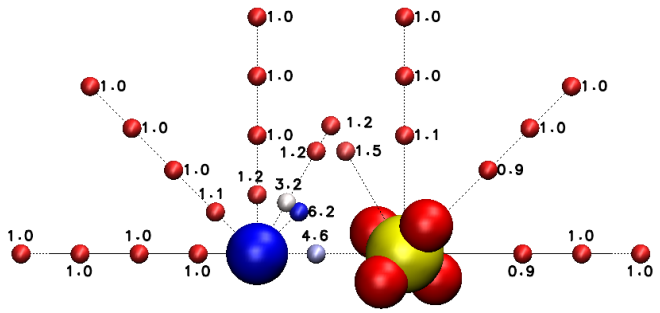

(a) Cooperative slowdown factors for OH rotation, $f_{c,OH}$.

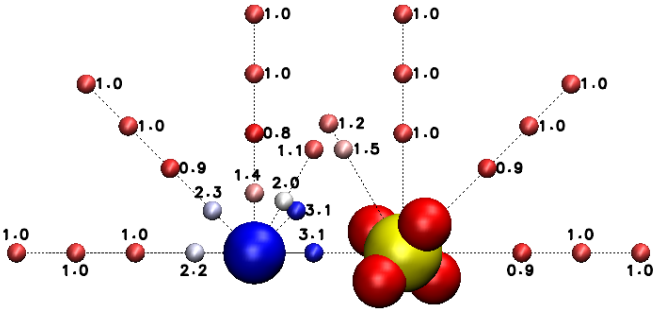

(b) Cooperative slowdown factors for dipole rotation, $f_{c,dip}$.

Figure 6: Reorientation dynamics of different water subpopulations near a single Mg^{2+}-SO_4^{2-} pair at $D = 5$ Å separation. The numbers next to the small spheres represent the cooperative slowdown factors, $f_{c,x}$, calculated using Equation 2. The color of the small spheres in each panel encodes the magnitude of the cooperative slowdown factor. Consecutive water subpopulations along the dotted lines are 1 or 2 Å apart.

first hydration layer. Third, for a 5 Å Mg^{2+}-SO_4^{2-} separation, our results indicate that intense cooperative slowdown of water rotation is largely limited to the first hydration layer of Mg^{2+}. Long-range cooperative slowdown is present up to $d = 6$ Å, corresponding to water molecules in the second hydration layer of SO_4^{2-} and the third hydration layer of Mg^{2+}, but this effect is significantly weaker ($f_c = 1.2$). At this short anion-cation separation, the much less densely charged Cs^+-Cl^- ions also cooperatively slow down water rotation. Cooperative slowdown in the Cs^+-Cl^- systems is, however, much weaker than that observed for Mg^{2+}-SO_4^{2-} in both magnitude of the cooperative slowdown and in the spatial range of the affected water subpopulations. As shown in Figure 7, Cs^+-Cl^- pairs induce a maximum cooperative slowdown factor $f_{c,OH} = 2.2$ for OH rotation (Figure 7(a)) and $f_{c,dip} = 1.9$ for

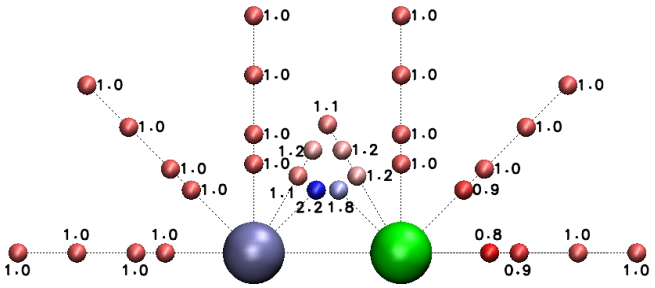

(a) Cooperative slowdown factors for OH rotation, $f_{c,OH}$.

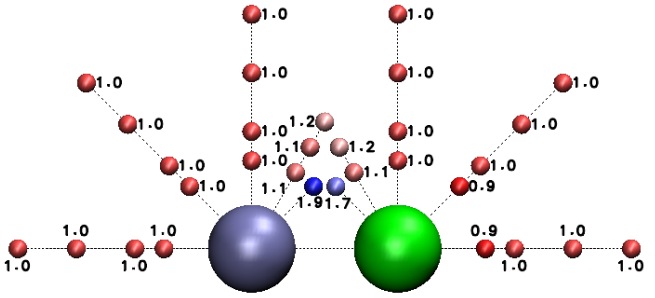

(b) Cooperative slowdown factors for dipole rotation, $f_{c,dip}$.

Figure 7: Reorientation dynamics of different water subpopulations near a single Cs^+-Cl^- pair at $D = 5$ Å separation. The numbers next to the small spheres represent the cooperative slowdown factors, $f_{c,x}$, calculated using Equation 2. The color of the small spheres in each panel encodes the magnitude of the cooperative slowdown factor. Consecutive water subpopulations along the dotted lines are 1 or 2 Å apart.

dipole rotation (Figure 7(b)), and cooperatively slow down only those water subpopulations between the ions ($\theta < 45°$) and belonging to the first hydration shell of either ion. The less noticeable cooperative slowdown of water rotation observed for cesium chloride is consistent with experiment[20,23,27]. Water reorientation behavior for systems with 6, 7, and 8 Å anion-cation separations, shown in the Supporting Information, interpolates between the behavior found for 12 and 5 Å as displayed in Figures 4 and 6 for magnesium sulfate, and Figures 5 and 7 for cesium chloride.

A possible origin for the cooperative slowdown of water rotation by pairs of ions is an increase in the magnitude of the electric field in their vicinity, relative to the electric field created by isolated ions. We investigate this possibility by looking for correlations between the cooperative slowdown factors of water subpopulations near ion pairs, and the ratio of the

electric field experienced by those subpopulations to that experienced by the corresponding subpopulation near isolated ions, E/E_{isol}. Results, shown in the Supporting Information, demonstrate that the weak cooperative slowdown induced by a single pair of ions that are 10 or 12 Å apart indeed correlates with changes in the ratio E/E_{isol}, suggesting it is caused by a non-specific electric field effect. The marked cooperative slowdown effect observed in systems with shorter anion-cation separations, however, shows no such correlation. A more detailed study of the physical mechanisms leading to cooperative slowdown is in preparation.

The results described thus far shed light onto cooperative effects in solutions of low to moderate concentration. At higher concentrations, however, pairs of ions are not isolated but instead exist in the vicinity of other ions. To assess the differences in water dynamics between systems with individual ion pairs and systems with multiple, nearby, pairs of ions, we investigate the multi-ion system shown in Figure 1(b). This system has effective concentration $3.6m$ but consists of multiple layers of ions at fixed positions. We emphasize that, because the ions are fixed, the results should be interpreted qualitatively only, and direct comparisons with experiment are not meaningful. Simulations with free ions could not be performed because appropriate parameters for the interactions between Mg^{2+} and SO_4^{2-} are not yet available.

We calculate $P_{2,x}(t)$ for the two water subpopulations shown in Figure 1(b): the ensemble of water molecules that at $t = 0$ are at a minimum distance of $d = 3 \pm 0.5$ or $d = 5 \pm 0.5$ Å from the ions. As for the other systems, we fit a sum of three exponentials to the resulting curves and calculate the average decay times. The average decay times and corresponding cooperative slowdown times for OH or dipole reorientation of these water subpopulations are given in Table 1. The cooperative slowdown factors are calculated taking as reference the decay times of the isolated SO_4^{2-} ion for $d = 3$ and $d = 5$ Å tabulated in the Supporting Information. For comparison, in Table 1 we also show the cooperative slowdown factors for the analogous subpopulations in systems with a single pair of ions: the (SO_4^{2-},3Å,0°) subpopulation in the system with Mg^{2+}-SO_4^{2-} separation $D = 6$ Å, and the (SO_4^{2-},5Å,0°)

subpopulation in the system with $D = 10$ Å. These results show that cooperative slowdown factors for the multi-ion system are two to seven times larger than in the system with single ion pairs. This trend hints at the possibility that cooperative slowdown in concentrated solutions is more than the sum of the cooperative slowdown induced by individual pairs of ions, instead resulting from a collective effect of ions. Simulations with free ions, using improved models that adequately reproduce ion-ion interactions, will be necessary to gain further insight into water reorientation in concentrated ion solutions.

Table 1: Cooperative slowdown factors, $f_{c,x}^{mi}$, for the reorientation of OH groups or water dipoles, for water subpopulations that at $t = 0$ are at a minimum distance $d = 3 \pm 0.5$ or $d = 5 \pm 0.5$ Å from the ions in a multi-ion (mi) Mg^{2+}-SO_4^{2-} system, as shown in Figure 1(b). For comparison, the cooperative slowdown factors for analogous water subpopulations in systems with single ion pairs, $f_{c,x}$, are also shown. All cooperative slowdown factors are calculated taking as reference the SO_4^{2-} ion.

Water subpopulation	τ_{dip}^{mi} (ps)	$f_{c,dip}^{mi}$	$f_{c,dip}$	τ_{OH}^{mi} (ps)	$f_{c,OH}^{mi}$	$f_{c,OH}$
$d = 3$ Å	49.8	17.9	2.6	38.4	11.4	2.9
$d = 5$ Å	4.5	2.3	1.2	5.2	2.6	1.1

4. Concluding Remarks

Our results are consistent with a scenario where individual pairs of anions and cations in solution – abundant species at low to moderate salt concentrations – cooperatively slow down water rotation. The identity of the cation and the anion affect both the spatial extent over which water molecules are slowed down and the magnitude of the slowdown. Moderate to strong cooperative slowdown is observed when cesium chloride and magnesium sulfate are in solvent-shared or solvent-separated ion pair configurations, but is limited to the first hydration shell of the ions. Long-range cooperative slowdown effects, extending as far as 6 Å from the ions, are observed for the densely charged magnesium sulfate ions but the magnitude of the slowdown and the number of affected water molecules is small. These results imply that the largest cooperative slowdown of water rotation should be observed

for salts of densely charged anions and cations with dissimilar sizes, because these salts preferentially form solvent-shared and solvent-separated ion pairs at the expense of contact ion pairs[82,83], a connection that other authors have also hinted at from simulations with artificial monovalent ion systems[26].

As mentioned above, different experiments disagree on the spatial range of the cooperative effect, with some suggesting that it is long-range whereas others that it is limited to the first hydration layer of the ions. For solutions of moderate concentration, our results support the latter view, and suggest a possible way to reconcile the two sets of experiments. As described above, a long-range cooperative effect was suggested from fs-IR experiments analyzed using a two-population model which considers two populations of water molecules with bulk-like or slow dynamics, with reorientation times 2.6 ps and 10 ps, respectively. These times are taken to be the same for all salt solutions irrespective of composition or concentration. In contrast, our results show that these reorientation times are strongly salt-dependent and, in addition, vary significantly with the ion-ion separation. Better estimates for the spatial range of cooperative slowdown may be obtained from experiments by using models that reflect our findings.

More generally, our results do not support the notion that the Hofmeister series is primarily due to long-range effects of ions on water properties. Instead, they point to the possibility that models of ion solvation may focus primarily on the first hydration layer without excessive loss of accuracy. Prior work on coarse-grained models of solvent-free ionic solutions, based on the Generalized Langevin Equation, suggest this expectation is warranted for the case of monovalent salts like NaCl: the ion-ion memory kernels for the GLE have been shown to differ between contact, solvent-shared and solvent-separated ion pair configurations[84], but should not vary strongly for larger interionic separations, as suggested by the fact that good agreement between GLE and all-atom simulations can be obtained for low to moderate ionic concentrations using neither distance-dependent nor concentration-dependent memory kernels[85]. Our results on magnesium sulfate point to the possibility that an adequate de-

scription of ion dynamics in systems with multivalent ions might require distance-dependent memory kernels even at relatively low concentrations, because of the larger effect of these ions on water dynamics relatively to monovalent ones, but that this distance-dependence need not extend beyond solvent-shared ion pair configurations.

Acknowledgement

AVV thanks Dr. R. Kramer Campen for stimulating discussions on the topic. We thank an anonymous reviewer for interesting suggestions regarding the impact of our results on the development of coarse-grained models of ion solvation.

Supporting Information Available

Details of sulfate parameterization, ion-water radial distribution functions, residence and reorientation times of water near isolated ions, cooperative slowdown factors of all systems, correlation between cooperative slowdown factors and the electric field. This material is available free of charge via the Internet at `http://pubs.acs.org/`.

References

(1) Collins, K. D.; Washabaugh, M. W. The Hofmeister Effect and the Behaviour of Water at Interfaces. *Q. Rev. Biophys.* **1985**, *18*, 323–422.

(2) Cacace, M. G.; Landau, E. M.; Ramsden, J. J. The Hofmeister Series: Salt and Solvent Effects on Interfacial Phenomena. *Q. Rev. Biophys.* **1997**, *30*, 241–277.

(3) Pegram, L. M.; Record, J., M. Thomas Hofmeister Salt Effects on Surface Tension Arise from Partitioning of Anions and Cations Between Bulk Water and the Air-Water Interface. *J. Phys. Chem. B* **2007**, *111*, 5411–5417.

(4) Zangi, R. Can Salting-In/Salting-Out Ions be Classified as Chaotropes/Kosmotropes? *J. Phys. Chem. B* **2009**, *114*, 643–650.

(5) He, Y.; Shao, Q.; Chen, S.; Jiang, S. Water Mobility: A Bridge Between the Hofmeister Series of Ions and the Friction of Zwitterionic Surfaces in Aqueous Environments. *J. Phys. Chem. C* **2011**, *115*, 15525–15531.

(6) Gibb, C. L. D.; Gibb, B. C. Anion Binding to Hydrophobic Concavity Is Central to the Salting-in Effects of Hofmeister Chaotropes. *J. Am. Chem. Soc.* **2011**, *133*, 7344–7347.

(7) Otten, D. E.; Shaffer, P. R.; Geissler, P. L.; Saykally, R. J. Elucidating the Mechanism of Selective Ion Adsorption to the Liquid Water Surface. *Proc. Natl. Acad. Sci. USA* **2012**, *109*, 701–705.

(8) Koneshan, S.; Rasaiah, J. C.; Lynden-Bell, R. M.; Lee, S. H. Solvent Structure, Dynamics, and Ion Mobility in Aqueous Solutions at 25 Degrees C. *J. Phys. Chem. B* **1998**, *102*, 4193–4204.

(9) Cappa, C. D.; Smith, J. D.; Wilson, K. R.; Messer, B. M.; Gilles, M. K.; Cohen, R. C.; Saykally, R. J. Effects of Alkali Metal Halide Salts on the Hydrogen Bond Network of Liquid Water. *J. Phys. Chem. B* **2005**, *109*, 7046–7052.

(10) Marcus, Y.; Hefter, G. Ion Pairing. *Chem. Rev.* **2006**, *106*, 4585–4621.

(11) Tanwar, A.; Bagchi, B.; Pal, S. Interaction Induced Shifts in O-H Stretching Frequency of Water in Halide-Ion Water Clusters: A Microscopic Approach With a Bond Descriptor. *J. Chem. Phys.* **2006**, *125*, 214304.

(12) Collins, K. D. Ion Hydration: Implications for Cellular Function, Polyelectrolytes, and Protein Crystallization. *Biophys. Chem.* **2006**, *119*, 271–281.

(13) Wachter, W.; Fernandez, S.; Buchner, R.; Hefter, G. Ion Association and Hydration in

Aqueous Solutions of LiCl and Li_2SO_4 by Dielectric Spectroscopy. *J. Phys. Chem. B* **2007**, *111*, 9010–9017.

(14) Bakker, H. J. Structural Dynamics of Aqueous Salt Solutions. *Chem. Rev.* **2008**, *108*, 1456–1473.

(15) Smith, J. D.; Saykally, R. J.; Geissler, P. L. The Effects of Dissolved Halide Anions on Hydrogen Bonding in Liquid Water. *J. Am. Chem. Soc.* **2007**, *129*, 13847–13856.

(16) Marcus, Y. Effect of Ions on the Structure of Water: Structure Making and Breaking. *Chem. Rev.* **2009**, *109*, 1346–1370.

(17) Lin, Y. . S.; Auer, B. M.; Skinner, J. L. Water Structure, Dynamics, and Vibrational Spectroscopy in Sodium Bromide Solutions. *J. Chem. Phys.* **2009**, *131*, 144511.

(18) O'Brien, J. T.; Prell, J. S.; Bush, M. F.; Williams, E. R. Sulfate Ion Patterns Water at Long Distance. *J. Am. Chem. Soc.* **2010**, *132*, 8248–8249.

(19) Prell, J. S.; O'Brien, J. T.; Williams, E. R. Structural and Electric Field Effects of Ions in Aqueous Nanodrops. *J. Am. Chem. Soc.* **2011**, *133*, 4810–4818.

(20) Funkner, S.; Niehues, G.; Schmidt, D. A.; Heyden, M.; Schwaab, G.; Callahan, K. M.; Tobias, D. J.; Havenith, M. Watching the Low-Frequency Motions in Aqueous Salt Solutions: The Terahertz Vibrational Signatures of Hydrated Ions. *J. Am. Chem. Soc.* **2012**, *134*, 1030–1035.

(21) Irudayam, S. J.; Henchman, R. H. Long-Range Hydrogen-Bond Structure in Aqueous Solutions and the Vapor-Water Interface. *J. Chem. Phys.* **2012**, *137*, 034508.

(22) Tielrooij, K. J.; Garcia-Araez, N.; Bonn, M.; Bakker, H. J. Cooperativity in Ion Hydration. *Science* **2010**, *328*, 1006–1009.

(23) van der Post, S. T.; Bakker, H. J. The Combined Effect of Cations and Anions on the Dynamics of Water. *PCCP* **2012**, *14*, 6280–6288.

(24) Omta, A. W.; Kropman, M. F.; Woutersen, S.; Bakker, H. J. Negligible Effect of Ions on the Hydrogen-Bond Structure in Liquid Water. *Science* **2003**, *301*, 347–349.

(25) Giammanco, C. H.; Wong, D. B.; Fayer, M. D. Water Dynamics in Divalent and Monovalent Concentrated Salt Solutions. *J. Phys. Chem. B* **2012**, *116*, 13781–13792.

(26) Yang, L.; Fan, Y.; Gao, Y. Q. Differences of Cations and Anions: Their Hydration, Surface Adsorption, and Impact on Water Dynamics. *J. Phys. Chem. B* **2011**, *115*, 12456–12465.

(27) Tielrooij, K. J.; van der Post, S. T.; Hunger, J.; Bonn, M.; Bakker, H. J. Anisotropic Water Reorientation Around Ions. *J. Phys. Chem. B* **2011**, *115*, 12638–12647.

(28) dos Santos, A. P.; Levin, Y. Ion Specificity and the Theory of Stability of Colloidal Suspensions. *Phys. Rev. Lett.* **2011**, *106*, 167801–.

(29) Levin, Y.; dos Santos, A. P.; Diehl, A. Ions at the Air-Water Interface: An End to a Hundred-Year-Old Mystery? *Phys. Rev. Lett.* **2009**, *103*, 257802–.

(30) Cao, Z.; Dama, J. F.; Lu, L.; Voth, G. A. Solvent Free Ionic Solution Models from Multiscale Coarse-Graining. *J. Chem. Theory Comput.* **2013**, *9*, 172–178.

(31) Roy, S.; Mitra, I.; Llinas, R. Non-Markovian Noise Mediated Through Anomalous Diffusion Within Ion Channels. *Physical Review E* **2008**, *78*, 041920.

(32) Gordon, D.; Krishnamurthy, V.; Chung, S.-H. Generalized Langevin Models of Molecular Dynamics Simulations With Applications to Ion Channels. *J. Chem. Phys.* **2009**, *131*, 134102–134102.

(33) Jiao, D.; King, C.; Grossfield, A.; Darden, T. A.; Ren, P. Simulation of Ca^{2+} and Mg^{2+} Solvation using Polarizable Atomic Multipole Potential. *J. Phys. Chem. B* **2006**, *110*, 18553–18559.

(34) Wernersson, E.; Jungwirth, P. Effect of Water Polarizability on the Properties of Solutions of Polyvalent Ions: Simulations of Aqueous Sodium Sulfate with Different Force Fields. *J. Chem. Theory Comput.* **2010**, *6*, 3233–3240.

(35) Yoo, J.; Aksimentiev, A. Improved Parametrization of Li^+, Na^+, K^+, and Mg^{2+} Ions for All-Atom Molecular Dynamics Simulations of Nucleic Acid Systems. *J. Phys. Chem. Lett.* **2012**, *3*, 45–50.

(36) Lamoureux, G.; Harder, E.; Vorobyov, I. V.; Roux, B.; MacKerell Jr., A. D. A Polarizable Model of Water for Molecular Dynamics Simulations of Biomolecules. *Chem. Phys. Lett.* **2006**, *418*, 245–249.

(37) Yu, H.; Whitfield, T. W.; Harder, E.; Lamoureux, G.; Vorobyov, I.; Anisimov, V. M.; MacKerell, J., Alexander D.; Roux, B. Simulating Monovalent and Divalent Ions in Aqueous Solution Using a Drude Polarizable Force Field. *J. Chem. Theory Comput.* **2010**, *6*, 774–786.

(38) Marcus, Y. *Ion Properties*; Marcel Dekker, Inc.: New York, USA, 1997.

(39) Cannon, W. R.; Pettitt, B. M.; McCammon, J. A. Sulfate Anion in Water: Model Structural, Thermodynamic, and Dynamic Properties. *J. Phys. Chem.* **1994**, *98*, 6225–6230.

(40) Ishiyama, T.; Morita, A. Molecular Dynamics Simulation of Sum Frequency Generation Spectra of Aqueous Sulfuric Acid Solution. *J. Phys. Chem. C* **2011**, *115*, 13704–13716.

(41) Jungwirth, P.; Curtis, J. E.; Tobias, D. J. Polarizability and Aqueous Solvation of the Sulfate Dianion. *Chem. Phys. Lett.* **2003**, *367*, 704–710.

(42) Serr, A.; Netz, R. R. Polarizabilities of Hydrated and free Ions derived from DFT Calculations. *Int. J. Quantum Chem.* **2006**, *106*, 2960–2974.

(43) Horinek, D.; Mamatkulov, S. I.; Netz, R. R. Rational design of Ion Force Fields based on thermodynamic Solvation Properties. *J. Chem. Phys.* **2009**, *130*, 124507.

(44) Warren, G. L.; Patel, S. Hydration Free Energies of Monovalent Ions in Transferable Intermolecular Potential Four Point Fluctuating Charge Water: An Assessment of Simulation Methodology and Force Field Performance and Transferability. *J. Chem. Phys.* **2007**, *127*, 064509–19.

(45) Hünenberger, P.; Reif, M. In *Single-ion Solvation - experimental and theoretical approaches to elusive thermodynamic quantities*; Hirst, J., Jordan, K., Lim, C., Thiel, W., Eds.; RSC Theoretical and Computational Chemistry Series; RSC, 2011.

(46) Bhattacharjee, A.; Pribil, A. B.; Randolf, B. R.; Rode, B. M.; Hofer, T. S. Hydration of Mg^{2+} and its Influence on the Water Hydrogen Bonding Network Via Ab Initio QMCF MD. *Chem. Phys. Lett.* **2012**, *536*, 39–44.

(47) Ge, L.; Bernasconi, L.; Hunt, P. Linking Electronic and Molecular Structure: Insight Into Aqueous Chloride Solvation. *PCCP* **2013**, *15*, 13169.

(48) Tanaka, K. Measurements of Tracer Diffusion Coefficients of Sulphate Ions in Aqueous Solutions of Ammonium Sulphate and Sodium Sulphate, and of Water in Aqueous Sodium Sulphate Solutions. *J. Chem. Soc., Faraday Trans. 1* **1988**, *84*, 2895–2897.

(49) Ohtaki, H.; Radnai, T. Structure and Dynamics of Hydrated Ions. *Chem. Rev.* **1993**, *93*, 1157–1204.

(50) Vchirawongkwin, V.; Rode, B. M.; Persson, I. Structure and Dynamics of Sulfate Ion in Aqueous Solution - An Ab Initio QMCF MD Simulation and Large Angle X-ray Scattering Study. *J. Phys. Chem. B* **2007**, *111*, 4150–4155.

(51) Pegado, L.; Marsalek, O.; Jungwirth, P.; Wernersson, E. Solvation and Ion-Pairing

Properties of the Aqueous Sulfate Anion: Explicit Versus Effective Electronic Polarization. *PCCP* **2012**, *14*, 10248–10257.

(52) Buchner, R.; Chen, T.; Hefter, G. Complexity in Simple Electrolyte Solutions: Ion Pairing in $MgSO_{4\ (aq)}$. *J. Phys. Chem. B* **2004**, *108*, 2365–2375.

(53) Klasczyk, B.; Knecht, V. Kirkwood-Buff Derived Force Field for Alkali Chlorides in Simple Point Charge Water. *J. Chem. Phys.* **2010**, *132*, 024109.

(54) Luo, Y.; Jiang, W.; Yu, H.; MacKerell, A. D.; Roux, B. Simulation Study of Ion Pairing in Concentrated Aqueous Salt Solutions With a Polarizable Force Field. *Faraday Discuss.* **2013**, *160*, 135–149.

(55) Callahan, K. M.; Casillas-Ituarte, N. N.; Roeselova, M.; Allen, H. C.; Tobias, D. J. Solvation of Magnesium Dication: Molecular Dynamics Simulation and Vibrational Spectroscopic Study of Magnesium Chloride in Aqueous Solutions. *J. Phys. Chem. A* **2010**, *114*, 5141–5148.

(56) Fyta, M.; Kalcher, I.; Dzubiella, J.; Vrbka, L.; Netz, R. R. Ionic Force Field Optimization Based on Single-Ion and Ion-Pair Solvation Properties. *J. Chem. Phys.* **2010**, *132*, 024911.

(57) Fyta, M.; Netz, R. R. Ionic Force Field Optimization Based on Single-Ion and Ion-Pair Solvation Properties: Going Beyond Standard Mixing Rules. *J. Chem. Phys.* **2012**, *136*, 124103–11.

(58) Larson, J. W. Thermodynamics of Divalent Metal Sulfate Dissociation and Structure of Solvated Metal Sulfate Ion Pair. *J. Phys. Chem.* **1970**, *74*, 3392–3396.

(59) Daly, F. P.; Kester, D. R.; Brown, C. W. Sodium and Magnesium Sulfate Ion Pairing - Evidence From Raman Spectroscopy. *J. Phys. Chem.* **1972**, *76*, 3664–3668.

(60) Davis, A. R.; Oliver, B. G. Raman Spectroscopic Evidence For Contact Ion-pairing in Aqueous Magnesium Sulfate Solutions. *J. Phys. Chem.* **1973**, *77*, 1315–1316.

(61) Rudolph, W. W.; Irmer, G.; Hefter, G. T. Raman Spectroscopic Investigation of Speciation in $MgSO_{4\ (aq)}$. *PCCP* **2003**, *5*, 5253–5261.

(62) Phillips, J. C.; Braun, R.; Wang, W.; Gumbart, J.; Tajkhorshid, E.; Villa, E.; Chipot, C.; Skeel, R. D.; Kale, L.; Schulten, K. Scalable Molecular Dynamics With NAMD. *J. Comput. Chem.* **2005**, *26*, 1781–1802.

(63) Humphrey, W.; Dalke, A.; Schulten, K. VMD: Visual Molecular Dynamics. *J. Mol. Graphics* **1996**, *14*, 33–38.

(64) Jiang, W.; Hardy, D. J.; Phillips, J. C.; MacKerell, A. D.; Schulten, K.; Roux, B. High-Performance Scalable Molecular Dynamics Simulations of a Polarizable Force Field Based on Classical Drude Oscillators in NAMD. *J. Phys. Chem. Lett.* **2010**, *2*, 87–92.

(65) Miyamoto, S.; Kollman, P. A. Settle: An Analytical Version of the SHAKE and RATTLE Algorithm for Rigid Water Models. *J. Comput. Chem.* **1992**, *13*, 952–962.

(66) Wood, W. W. In *Physics of simple Liquids*; Temperley, H. N. V., S., R. J., S., R. G., Eds.; North-Holland publishing company - Amsterdam, 1968; Chapter 5, pp 151–155.

(67) Chitra, R.; Yashonath, S. Estimation of Error in the Diffusion Coefficient from Molecular Dynamics Simulations. *J. Phys. Chem. B* **1997**, *101*, 5437–5445.

(68) Lin, Y. S.; Pieniazek, P. A.; Yang, M.; Skinner, J. L. On the Calculation of Rotational Anisotropy Decay, as Measured by Ultrafast Polarization-Resolved Vibrational Pump-Probe Experiments. *J. Chem. Phys.* **2010**, *132*, 174505.

(69) Laage, D.; Hynes, J. T. Do More Strongly Hydrogen-Bonded Water Molecules Reorient More Slowly? *Chem. Phys. Lett.* **2006**, *433*, 80–85.

(70) Vila Verde, A.; Campen, R. K. Disaccharide Topology Induces Slowdown in Local Water Dynamics. *J. Phys. Chem. B* **2011**, *115*, 7069–7084.

(71) Vila Verde, A.; Bolhuis, P. G.; Campen, R. K. Statics and Dynamics of Free and Hydrogen-Bonded OH Groups at the Air/Water Interface. *J. Phys. Chem. B* **2012**, *116*, 9467–9481.

(72) Moilanen, D. E.; Fenn, E. E.; Lin, Y.-S.; Skinner, J. L.; Bagchi, B.; Fayer, M. D. Water Inertial Reorientation: Hydrogen Bond Strength and the Angular Potential. *Proc. Natl. Acad. Sci. USA* **2008**, *105*, 5295–5300.

(73) Laage, D.; Hynes, J. T. A Molecular Jump Mechanism of Water Reorientation. *Science* **2006**, *311*, 832–835.

(74) Laage, D.; Hynes, J. T. On the Molecular Mechanism of Water Reorientation. *J. Phys. Chem. B* **2008**, *112*, 14230–14242.

(75) Laage, D.; Stirnemann, G.; Hynes, J. T. Why Water Reorientation Slows Without Iceberg Formation Around Hydrophobic Solutes. *J. Phys. Chem. B* **2009**, *113*, 2428–2435.

(76) Laage, D.; Stirnemann, G.; Sterpone, F.; Rey, R.; Hynes, J. T. Reorientation and Allied Dynamics in Water and Aqueous Solutions. *Annu. Rev. Phys. Chem.* **2011**, *62*, 395–416.

(77) Stirnemann, G.; Rossky, P. J.; Hynes, J. T.; Laage, D. Water Reorientation, Hydrogen-Bond Dynamics and 2D-IR Spectroscopy Next to an Extended Hydrophobic Surface. *Faraday Discuss.* **2010**, *146*, 263–281.

(78) Stirnemann, G.; Sterpone, F.; Laage, D. Dynamics of Water in Concentrated Solutions of Amphiphiles: Key Roles of Local Structure and Aggregation. *J. Phys. Chem. B* **2011**, *115*, 3254–3262.

(79) Stirnemann, G.; Castrillón, S. R.-V.; Hynes, J. T.; Rossky, P. J.; Debenedetti, P. G.; Laage, D. Non-Monotonic Dependence of Water Reorientation Dynamics on Surface Hydrophilicity: Competing Effects of the Hydration Structure and Hydrogen-Bond Strength. *PCCP* **2011**, *13*, 19911–19917.

(80) Kurisaki, I.; Takahashi, T. Assessment of Dynamic Properties of Water Around a Monovalent Ion: A Classical Molecular Dynamics Simulation Study. *Comp. Theor. Chem.* **2011**, *966*, 26–30.

(81) van der Post, S. T.; Tielrooij, K.-J.; Hunger, J.; Backus, E. H. G.; Bakker, H. J. Femtosecond Study of the Effects of Ions and Hydrophobes on the Dynamics of Water. *Faraday Discuss.* **2013**, *160*, 171–189.

(82) Collins, K. D. Ions from the Hofmeister Series and Osmolytes: Effects on Proteins in Solution and in the Crystallization Process. *Methods* **2004**, *34*, 300–311.

(83) Fennell, C. J.; Bizjak, A.; Vlachy, V.; Dill, K. A. Ion Pairing in Molecular Simulations of Aqueous Alkali Halide Solutions. *J. Phys. Chem. B* **2009**, *113*, 6782–6791.

(84) Rey, R.; Guardia, E.; Padro, J. A. Friction Kernels For the Relative Dynamics of Ion-pairs In Water. *J. Chem. Phys.* **1992**, *97*, 1343–1352.

(85) Canales, M.; Sese, G. Generalized Langevin Dynamics Simulations of NaCl Electrolyte Solutions. *J. Chem. Phys.* **1998**, *109*, 6004–6011.

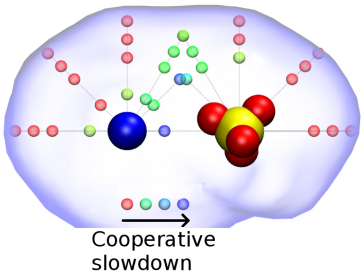

Figure 8: TOC graphic.